

Research Paper

Impact Behaviour of Safety Shoe High Strength Steel Parts

Nuno PEIXINHO, Sérgio COSTA, João MENDONÇA

Department of Mechanical Engineering
University of Minho
Guimarães, Portugal
e-mail: peixinho@dem.uminho.pt

This study presents results on the dynamic response of safety toe cap models made of high-strength steel. The structural response to impact loading conditions under normative requirements was properly related to tap the potential of lightweight design for significant reduction of thickness. A fully martensitic steel grade was selected, and numerical models were used to study extensive plastic deformation and strain-rate dependence. Material properties were modelled using the Cowper-Symonds models. The numerical simulation was developed using ANSYS explicit dynamics software and was compared to an experimental standard testing of final prototypes. The numerical modelling approach analysed different friction models seeking to better describe collapsing behaviour. A local stiffening toe cap model with high energy absorption efficiency was validated.

Key words: ultra-high-strength steel; impact loading; numerical simulation; safety toe cap.

1. INTRODUCTION

The toe cap as an active element of personal protective equipment (PPE) frequently used in the prevention of occupational accidents has evolved through a strict normative framework, where the structural functionality is of utmost relevance. In this study, the impact resistance test according to the European Standard EN ISO 20345:2010, which is the most demanding requirement for metal toe caps, was carried out.

The toe cap represents the most normative integrant component in safety footwear, with challenging requirements in structural and crash deformation resistance [1]. In addition, the toe cap is the heaviest element contributing to approximately 35% of the average weight of standard high performance footwear and several problems are inevitably associated with health, fatigue in extended use and occupational injuries [2–4]. Thus, structural design and material selection of safety toe caps have been assumed as multidisciplinary design trends,

with a division between metallic and polymeric composite models being postulated based on weight reduction research [4, 5].

These non-metallic solutions are currently lighter, as relevant studies on polymeric and hybrid models combined reinforced polyester composites with glass fibre and other advanced compounds for safety toe cap components reported a substantial weight reduction, in excess of 30%, compared with standard steel toe caps made of high carbon steel alloys (widely combined with specific heat treatments) [6–11]. Nevertheless, the main disadvantage of the non-metallic composites is associated with several constraints due to the stabilization of deformation responses for higher compression and impact load conditions. Commonly, composite toe cap solutions require a larger volume, owing to considerably larger thickness values to counterpoise higher rates of deformation and this affects in several ways their conception of fundamental integrant parts. In this context, an advanced metal solution made of ultra-high-strength steels was presented in [12] with a focus on their unique role in absorbing impact energy.

In this paper, a fully martensitic steel grade (Mart1200) was selected while one of the main objectives was to assess the influence of intermediate strain rates on crashworthy properties for an axial impact velocity of around 4 ms^{-1} . Experimental results of tensile testing of the selected steel grade were used to determine constitutive parameters and thus to simulate the impact behaviour of toe cap prototypes. For such purpose, material properties were modelled using the Cowper-Symonds model. The numerical simulation was developed using ANSYS explicit dynamics software and was extensively compared to an experimental standard testing of final prototypes. A local stiffening toe cap model with high energy absorption efficiency was validated.

2. EXPERIMENTAL SETUP

The test method comprises an impact apparatus incorporating a steel striker with a proper standard wedge of mass $(25 \pm 0.29) \text{ kg}$. The striker is adapted to fall freely on vertical guides from a controlled height to give the required impact energy of a minimum crash energy level of $200 \pm 4 \text{ J}$ to the upper toe cap surface. The Pegasil E-99 steel toe cap impact tester device (Zipor, Ltd.) was used in the experiments (Fig. 1). The clearance under the cap to a central area measurement, after the moment of impact, shall not be less than an appropriate value (that is, proportional to the model size) [1]. The time course of the load striker in the drop-impact test provides enough information to evaluate axial displacements, linear velocities, accelerations and consequently load and energy histories for the set of experiments. For such analysis, quantitative data was acquired by a high-speed Photron Ultima APX-RS video camera (Photron, Ltd.). The video sequences were recorded at 5000 fps for each experiment and then

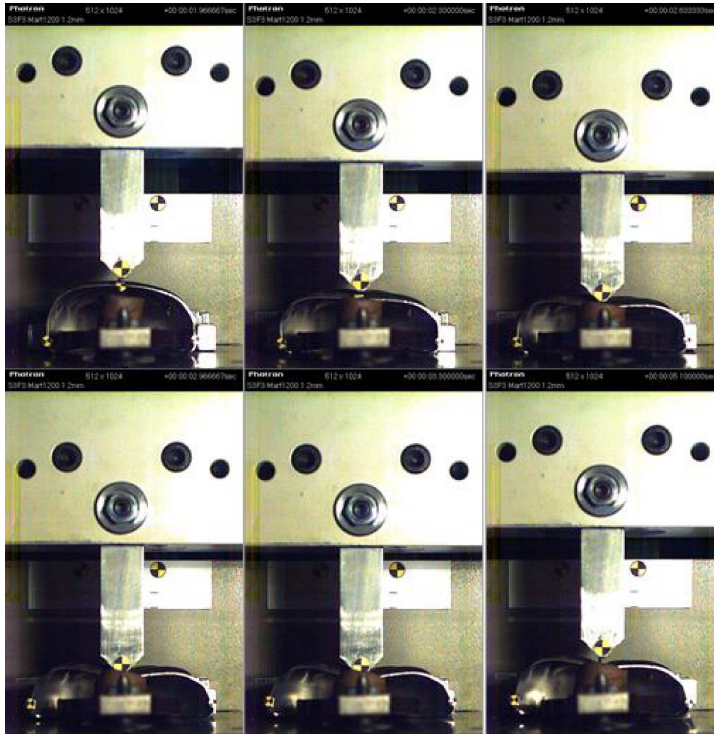


FIG. 1. Normative impact testing of prototype: sequence of high-speed film.

processed by an image tracking software TEMA Motion (Image Systems, Ltd.) (Fig. 1).

The experimental part of this study focused on the base geometric model S3F3b and the geometrically redesigned S3F3 model (Figs. 2b and 3), with all toe cap prototypes being of the same size and made of Mart1200 steel but with different thickness, as shown in Table 1. The main difference between these two geometries consisted in the ribs present in model S3F3, which aimed at providing additional stiffness and strength to support the demanding loading conditions. These caps with different geometries were analysed as optimised models with energy-absorbing properties. Developed by cold forming techniques, such models represent a conceptual approach of weight reduction in the order of 40% compared to conventional steel models.

3. NUMERICAL MODEL

The finite element analysis of the impact tests was carried out using the ANSYS explicit elasto-plastic finite element code, with the ANSYS Workbench

explicit dynamics module. Figure 2 presents the finite element model of the S3F3 geometric toe cap model, which is the focus of this study. The numerical model was developed using three independent parts: the representative striker body, a bottom layer for the constrained support of the toe cap, and the toe cap model on which the numerical analysis was performed. Impact velocities and mass values according to experimental testing were properly applied to the striker part. Its normative configuration in the contact region was considered, and the rest of the body was simplified in order to optimise the numerical model. Conditioning movement of the striker element was guaranteed regarding the development of guided displacement in the experimental impact test. A rigid body was considered, and a friction coefficient of the outer toe cap surface was applied.

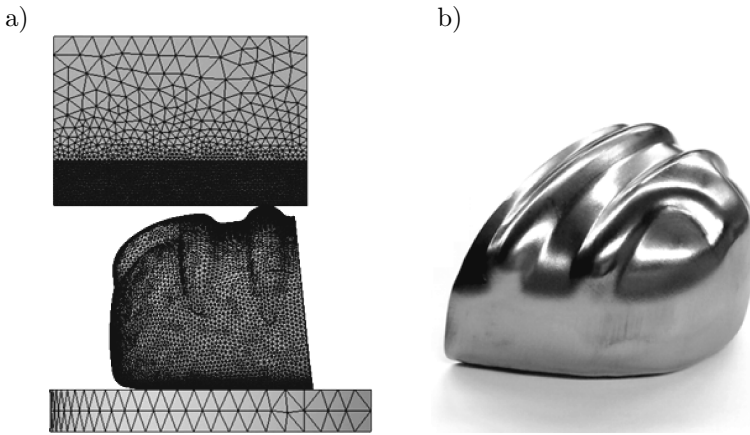


FIG. 2. a) Numerical model geometry, b) S3F3 model.

Friction parameters of the numerical simulation were analysed using different approaches, in which *friect.1* refers to an “unclamping mode” that restricts the interaction between the toe cap model and the bottom layer for the constrained support, whereas *friect.2* refers to controlled sliding at the base assuming the bottom layer is allowed (and with different friction coefficient parameters). Finally, *friect.4* refers to a bonded definition wherein the interface for the bottom layer is considered as totally clamped within body interactions.

The toe cap model was discretised into triangle-based prism elements with sizing mesh control, and the other solid parts were simplified using tetrahedral second-order structural solid elements with refinement on contact zones. The mesh sensitivity was studied to obtain run-time efficiency with desirable accuracy. Thus, a total mesh with skewness indicator for evaluation (mesh metric) of reference and an average value of 0.20 and a maximum value of 0.87 was taken.

Material models were characterised according to the constitutive parameters, and true stress-strain curves were introduced in tabular form into ANSYS for

base reference of the Cowper-Symonds model [13]. The strain-rate dependence data was introduced through parameters $D = 22521928.7 \text{ s}^{-1}$ and $q = 3.89$ as described in [13], being the set of material description parameters referenced in the current study as M12-CS6. In addition, other material properties were considered, e.g., $E = 207 \text{ GPa}$, $\nu = 0.3$, $\rho = 7830 \text{ kg/m}^3$.

4. EXPERIMENTAL AND NUMERICAL RESULTS

Figures 3 and 4 present selected deformed shapes resulting from the experimental impact tests. Figure 5 presents a comparison of load-time histories

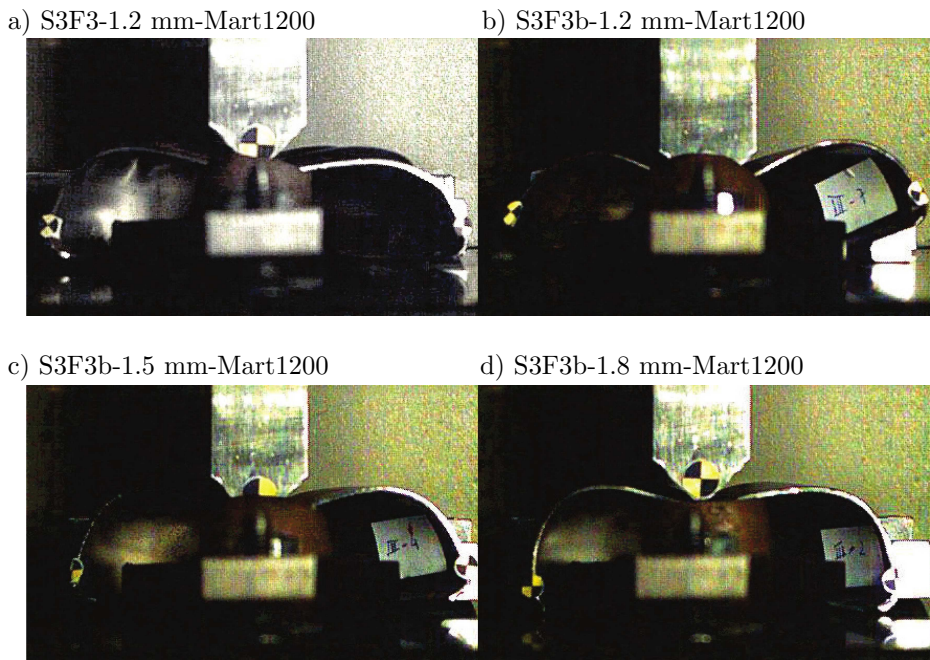


FIG. 3. Maximum deformed shapes observed during experimental test.

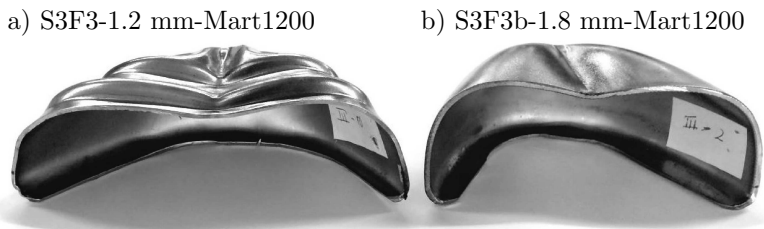


FIG. 4. Examples of final deformed shapes after experimental test.

of experimental tests for different prototypes. In Fig. 6, a comparison of load-time histories of the reference experimental test S3F3b-1.8 mm-Mart1200 and numerical simulations using the M12-CS6 and different interface parameters is presented. Table 1 presents a summary of numerical and experimental re-

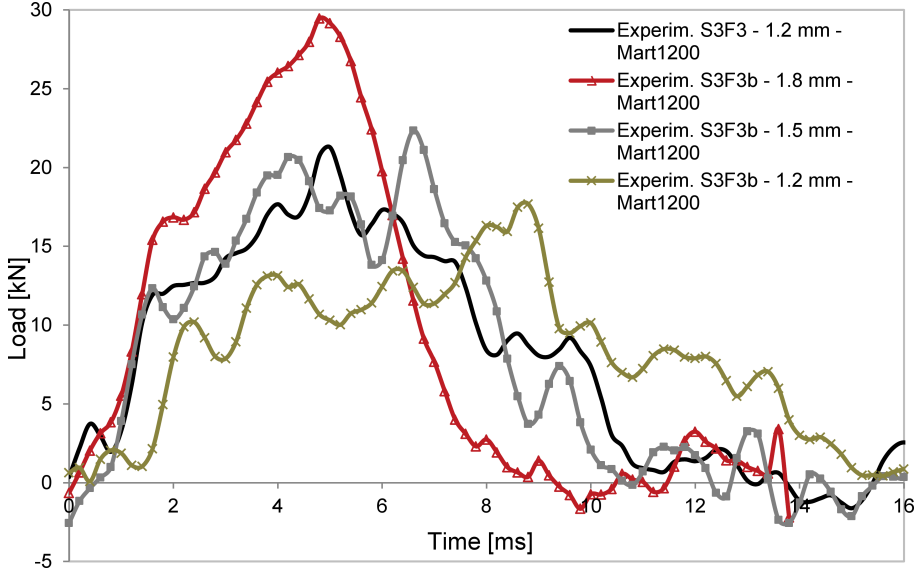


FIG. 5. Comparison of load-time histories of experimental tests for different prototypes.

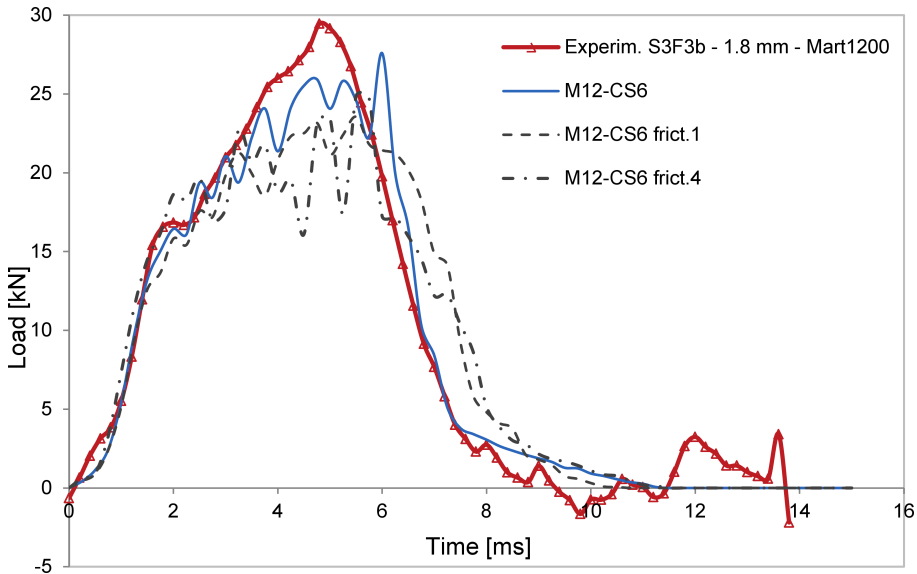


FIG. 6. Comparison of load-time histories of the reference experimental test S3F3b-1.8 mm-Mart1200 and numerical simulations using the M12-CS6 and different interface parameters.

sults and parameters. Differences are analysed through their influence on the final stiffening surface of 1.2 mm and a proper range of basic prototypes with different comparative thicknesses.

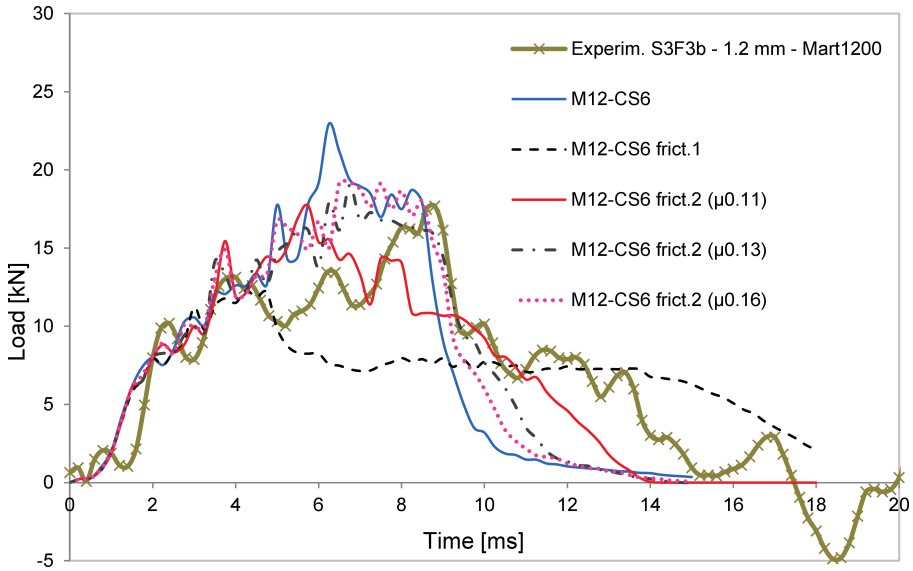


FIG. 7. Comparison of load-time histories of the experimental test and different numerical simulations using M12-CS6 on different interface parameters for the model S3F3b-1.2 mm-Mart1200.

Figure 3 suggests divergent experimental responses from the crash bodies. The biggest difference is observed between the following two geometries: final (a) and base (b), both of the same thickness. It becomes evident that the correction introduced by the ribbed areas took place at two levels: the acquired resistance in the central main region, where the impact contact is situated, and thus greater ability to minimize primary local damage is achieved, and second, the evolution of a dynamic mechanism of reaction for the complete structure, initiated, dependent and following the previous one, and confirmed by the deformation mode of the lateral support portions. For the same variable of material, the recognition of the lateral ribs' influence on cap response to impact is highlighted with intentional gliding actions of permanent contact on the tab-lower support interface, restraining therefore phenomena of greater instability. This is contrary to what is verified and substantiated in the base model S3F3b. The increase in thickness for other combinations of this base model led gradually to improved results, certainly a natural solving of problems of inertia resolved by the thickness ratio of the structural walls. Furthermore, it is relevant to compare a larger local impact damage produced in the 1.8 mm thick prototype with that of the thinner S3F3 prototype model.

Load histories in Fig. 5 and data in Table 1 compare the results for the set of prototypes covered by the experimental program. They had all passed the normative impact resistance test, except for S3F3b base model with a 1.2 mm thickness, which relates again to better performance variables of the S3F3 optimised prototype made of the same material and thickness as S3F3b. Furthermore, this reflects the performance extensively improved by the binomial high-strength material with proper structural design, and this is more so for the S3F3 series, as shown further.

When comparing both prototypes of 1.2 mm thickness, we see that the gap between their maximum (and mean) load responses is strictly related to the crushing displacement discrepancy and hence different approval status, as referred. The hardened surface of S3F3 has shown the improvement in crashworthy performance for all parameters.

Table 1. Experimental and numerical results.

Toe Cap Model <i>Specimen</i>	δ [mm]	MfA [mm]	P_{\max} [kN]	$E_a(A)$ [J]	$E_a(A)/w$ [J/kg]
S3F3-1.2 mm-Mart1200	17.54	(+)1.46	21.29	229.93	3504.96
S3F3b-1.2 mm-Mart1200	24.64	(-)5.44	17.68	174.63	2802.55
S3F3b-1.5 mm-Mart1200	17.66	(+)1.24	22.34	238.89	3048.22
S3F3b-1.8 mm-Mart1200	14.25	(+)4.40	29.46	253.89	2736.81
<i>S3F3b-1.2 mm-Mart1200</i>	<i>24.64</i>	<i>(-)5.44</i>	<i>17.68</i>	<i>174.63</i>	<i>2802.55</i>
M12-CS6	21.05	(-)1.71	22.95	219.49	3253.70
M12-CS6 frict. 1	27.21	(-)7.88	12.29	144.47	2141.57
M12-CS6 frict. 2 (μ 0.11)	22.14	(-)2.80	17.71	195.77	2902.00
M12-CS6 frict. 2 (μ 0.13)	21.67	(-)2.34	19.03	209.39	3103.96
M12-CS6 frict. 2 (μ 0.16)	21.45	(-)2.11	19.19	216.06	3202.80
<i>S3F3b-1.8 mm-Mart1200</i>	<i>14.25</i>	<i>(+)4.40</i>	<i>29.46</i>	<i>253.89</i>	<i>2736.81</i>
M12-CS6	14.83	(+)3.91	25.94	246.09	2501.46
M12-CS6 frict. 1	15.30	(+)3.44	23.56	241.64	2456.24
M12-CS6 frict. 4	14.77	(+)3.97	24.87	234.67	2385.40

δ – total crushing distance, MfA – margin for approval, P_{\max} – peak load, $E_a(A)$ – absorbed energy filtered only for the normative approval interval with positive performance.

Figures 6 and 7 present differences in the response of numerical prediction for the geometric base model between 1.8 mm and 1.2 mm thickness, using the same reference material M12-CS6. It is noted that the impact behaviour is quantitative and qualitatively simulated with diverging orientations. Therefore, some features and conclusions can be discussed, being mainly associated with previous considerations.

When analysing the application of 1.8 mm thick model, one can observe that the set of interface conditioning under study has performed relevant approximation with experimental results. The predictions modelled in this particular case have presented reasonable validation and seem appropriate to describe the structural impact behaviour of this combined prototype application without relevant variances.

It is worth noticing that the close values in all numerical predictions can be attributed to a weak dependence of strength increase for Mart1200 on initial strain rates, which apparently can be attributed to the fact that the present application model is thicker and hence induces less deformation. The strain rate, under these conditions of lower impact velocity, was reduced, and the stability of the deformation mode was not put to the test. In this context, the standard numerical conditions were accurate and performed the closest to values for peak load and energy absorption capacity, which reiterate, even in this model, the propensity to work under slippage events.

For the other base model of a 1.2 mm thickness, the results show a different response pattern in terms of numerical simulation. With a significant reduction of thickness and greater crush displacement values in the test, this may refer immediately to considerations previously observed for the increase of sensitivity and variation of strength properties with strain-rate dependence. The response to the impact simulation is possibly more pronounced, as the numerical values obtained for this application show an overestimated behaviour. The predicted values for crushing displacements are smaller and therefore, as observed in Fig. 7, the standard predicted load history produces higher mean and peak loads, compared with the experimental results.

Figure 7 presents results for different interface parameters. Here, a special attention was given to the lower frictional interface set, and further difficulties were found in the final definition of an adjusted collapse model, largely due to an increase of severe instability effects on deformation. The uncontrollable crash mode has created a critical barrier in the approach to the theoretically idealised prediction of total slip resistance release during the final stage of the test. Figure 7 highlights significant differences in maximum deformed shapes between subsequent interfaces' formulations observed in numerical tests. From the failure of an extreme folding mode performed by *friect.1*, the contribution of improved *friect.2*, with the in-between refinement of a dynamic frictional coefficient, seems relevant for qualitatively accurate numerical results. This set of conditions, to some limit, worked on a greater degree of freedom in the zone of contact in a controlled model of deformation, which allowed an improved approximation to the experimental results. Thus, Table 1 comprises results for the variant *friect.2* ($\mu 0.11$) that helped to decrease the difference between the experimental values, the load reaction in particular, and the approximated final

approved absorbed energy values. Nonetheless, the constraints imposed on the delineation of the best conditions, due to the critical moment for the transition into instability and associated with the own vulnerability of evolution for this base model, once more emphasize the benefit of performing the comparative test of the advanced ribbed S3F3 model in this context.

5. CONCLUSIONS

This study presented results on the dynamic response of safety toe cap models made of high-strength steel. A fully martensitic steel grade (Mart1200) was selected and numerical models for extensive plastic deformation and strain-rate dependence were developed using ANSYS explicit dynamics software. Numerical results were compared to experimental standard testing results of final prototypes. The comparison highlighted features associated with friction modelling and its importance for the simulated behaviour.

The experimental study emphasized the improvements of the ribbed S3F3 model regarding the base geometry. The acquired resistance in the main central region, where the impact contact is situated, provided a greater ability to minimize primary local damage, while the development of a dynamic mechanism of reaction for the entire structure was also improved.

The numerical models could generally simulate the impact test resistance of the case studies, in some cases with values of crashworthy properties close to experimental results. The set of interface conditioning under study has performed relevant approximation with experimental results, notably for the thickness of 1.8 mm. The analysis contributed to the validation of final prototypes with significant thickness reduction regarding the original model. The local stiffening toe cap model with high energy absorption efficiency was validated.

ACKNOWLEDGMENTS

The support from the Project S3 – Safety Slim Shoe, FCOMP-01-0202-FEDER-018458 and ICC – Lavoro is acknowledged. The authors would also like to thank the Swedish Steel AB for supplying the steel sheets and for technical support during the prototype forming process.

REFERENCES

1. European Committee for Standardization (CEN), EN 12568:2012, *Foot and leg protectors – Requirements and test methods for toecaps and penetration resistant inserts*, 2012.
2. CHIOU S.S., TURNER N., ZWIENER J., WEAVER D.L., HASKELL W.E., *Effect of boot weight and sole flexibility on gait and physiological responses of firefighters in stepping over*

- obstacles*, Human Factors: The Journal of the Human Factors and Ergonomics Society, **54**(3): 373–386, 2012, <http://journals.sagepub.com/doi/abs/10.1177/0018720811433464>.
3. TURNER N.L., CHIOU S., ZWIENER J., WEAVER D., SPAHR J., *Physiological effect of boot weight and design on men and women firefighters*, Journal of Occupational and Environmental Health, **7**(8): 477–482, 2010, <http://www.tandfonline.com/doi/abs/10.1080/15459624.2010.486285>.
 4. COSTA S.L., MENDONÇA J.P., PEIXINHO N., *Numerical simulation of quasi-static compression behavior of the toe cap component for safety footwear*, International Journal of Computer Theory & Engineering, **6**(4), 2014, <http://www.ijcte.org/index.php?m=content&c=index&a=show&catid=57&id=1047>.
 5. SAKUNDARINI N., TAHA Z., ABDUL-RASHID S.H., GHAZILA R.A.R., *Optimal multi-material selection for lightweight design of automotive body assembly incorporating recyclability*, Materials & Design, **50**: 846–857, 2013, <http://www.sciencedirect.com/science/article/pii/S0261306913002938>.
 6. LEE S.M., LIM T.S., *Damage tolerance of composite toecap*, Composite Structures, **67**(2): 167–174, 2005, <http://www.sciencedirect.com/science/article/pii/S0263822304003241>.
 7. KUHN M., NOWACKI J., HIMMEL N., *Development of an innovative high performance FRP protective toe cap*, Journal of Materials: Design and Applications, **219**(2): 91–109, 2005.
 8. DEKA L.J., BARTUS S.D., VAIDYA U.K., *Multi-site impact response of S2-glass/epoxy composite laminates*, Composites Science and Technology, **69**(6): 725–735, 2009, <http://www.sciencedirect.com/science/article/pii/S0266353808000857>.
 9. HO M.P., LAU K.T., *Design of an impact resistant glass fibre/epoxy composites using short silk fibres*, Materials & Design, **35**: 664–669, 2012, <http://www.sciencedirect.com/science/article/pii/S0261306911006959>.
 10. KURTH K.P., GROSBOL M., European Patent No. EP 2286686. Munich, Germany: European Patent Office, 2011.
 11. DAVOODI M.M., SAPUAN S.M., AHMAD D., ALI A., KHALINA A., JONOBI M., *Mechanical properties of hybrid kenaf/glass reinforced epoxy composite for passenger car bumper beam*, Materials & Design, **31**(10): 4927–4932, 2010, <http://www.sciencedirect.com/science/article/pii/S026130691000302X>.
 12. COSTA S.L., PEIXINHO N., MENDONÇA J.P., *Metal toe cap for safety footwear*, Patent application WO2015015477A1, 2015.
 13. COSTA S.L., MENDONÇA J.P., PEIXINHO N., *Study on the impact behaviour of a new safety toe cap model made of ultra-high-strength steels*, Materials & Design, **91**: 143–154, 2016, <https://www.sciencedirect.com/science/article/pii/S0264127515308248>.

Received December 26, 2017; accepted version February 12, 2018.
